Proceedings World Geothermal Congress 2023
Beijing, China, April 17 – 21, 2023

Analytical Study on Integrating Downhole Thermoelectric Power Generation with Coaxial Borehole Heat Exchanger in Geothermal Well

Junrong Liu[1],Yong Qiao[2], Kaiyuan Shi[1]

[1] School of Petroleum Engineering, China University of Petroleum (East China), Changjiang West Road 66, Huangdao District, Qingdao, PR China, 266580 ,[2] China Renewable Energy Engineering Institute, Liupukang North Street 2, Xicheng District, Beijing, PR China,100120

junrliu@upc.edu.cn

Keywords: Downhole Power Generation, Thermoelectric Module, Coaxial Borehole Heat Exchanger, Geothermal Well

ABSTRACT

Geothermal power generation with ORC technology is a traditional and popular way to utilize geothermal energy. A new design of downhole thermoelectric power generation combined with a coaxial borehole heat exchanger is proposed, where the geothermal well is isolated into power generation section and heat exchanging section from the top of the target zone with a packer. A cold fluid is injected to downhole through an insulation pipe, parts of the injected fluid flows reversely in casing-tubing annulus above the packer, and others flows into casing-tubing annulus below the packer and upwards in tubing. These flowing design provides cold source and hot source for thermoelectric generator, respectively. Analytical models of downhole temperature distribution for thermoelectric power generation are established. A case study for a geothermal well with 3000m length of power generation section and 500m length of heat exchanging section is performed. The results show that a substantial generating capacity could be realized with a higher wellhead temperature, and the payback period under different carbon tax scenarios is about 6 – 8 year. The proposed method realizes geothermal energy harvesting and power generation at the same time and can be operated all year round.

1. INTRODUCTION

Developing and utilizing geothermal energy is put forward as an urgent work and becomes one of important measures to solve the livelihood issues. Geothermal energy is a clean, renewable and sustainable energy. It is estimated that the Earth's total heat flux is about 44.2 ± 1.0 TW(Gando *et al.*, 2011). Geothermal energy will undoubtedly become an important part of the new energy in the future. Recently, geothermal power generation has developed rapidly. According to the statistics, the total installed geothermal power generation capacity in 2015 was 12,647 MWe. The annual electrical generation in 2019 was 92 TWh, approximately 1.0% of global electricity generation(IRENA, 2021). Nevertheless, the world's target by 2050 is to reach 1180 TWh of annual electricity generation from geothermal sources, which is about 2.5 to 3.1% of global electric demand (Goldstein *et al.*, 2011).

The power generation technology currently available in the geothermal industry depends on the reservoir properties (e.g. geological, geophysical, geochemical, physicochemical, thermodynamic, and others). Dry steam, flash (single, double and triple), and binary cycle power plants are three types of mature geothermal power generation technologies(DiPippo, 2008). Dry steam technology uses the vapor extracted from high temperature reservoir (> 240ºC) to produce electricity with a steam turbine and a generator. It is the cheapest geothermal generation process. Flash technology is usually used for liquid-vapor geothermal fluid, where a separation process is needed to generate power. The liquid-vapor separation process can include one, two or three stages, namely single-, double-, and triple-flash systems, respectively. The single-flash technology is generally used for the mixture with temperature over 210 ºC. The double-flash technology can increase both the efficiency of the process and the power generation in relation to the single-flash technology. The triple-flash technology is designed to utilize energy available in the brine coming from the double flash cycle. The binary cycle system is usually used for the geofluid produced from liquid-dominated reservoirs with temperatures lower than 200ºC. Due to the low temperature of the geofluid, a working fluid (which has a lower boiling point, e.g., n-isobutane, n-isopentane and pentane) is used to vaporize by the thermal energy in the geofluid to produce electricity with Organic Rankine Cycle (ORC) or Kalina cycle (Bertani, 2016, Tomasini-Montenegro *et al.*, 2017).

Many studies focused on the use of the borehole exchangers to extract geothermal heat (Wang *et al.*, 2009). It only extracts heat without producing mass (fluid) from the reservoir, so there are many advantages, such as reducing construction costs by eliminating surface facilities and dedicated injectors for brine disposal, avoiding surface subsidence, corrosion and scaling problems(Lund, 2003). Different designs of downhole heat exchanger were developed to harvest heat by different heat transfer mechanisms, such as conduction (Nalla *et al.*, 2004), natural convection(Wang *et al.*, 2009), and forced convection (Feng *et al.*, 2015). Morita et al(Morita *et al.*, 2005) proposed a Downhole Coaxial Heat Exchanger (DCHE) system combined with binary or Kalina cycles for exploitation of geothermal energy. Their results showed that 70kW power generation might be possible with a DCHE 2,000m deep. Noorollahi et al(Noorollahi *et al.*, 2016) studied the power generation from an abandoned geothermal well with depth of 3176m by circulating fluid in a coaxial double-pipe heat exchanger and using ammonia and isobutene as working fluids in binary cycle. The maximum net powers from the well are 270 kW and 181 kW for isobutane and ammonia with a mass flow rate of 12kg/s, respectively. Alimonti et al(Alimonti *et al.*, 2016) compared the thermal-to-electric conversion efficiency between the Organic Ranking Cycle (ORC) plant and the Stirling motor with wellbore heat exchanger. With the same working parameters, the net electric powers are 121kW for ORC and 152kW for Stirling motor.

A lot of geothermal resources found in the world belong to the low-temperature category, which are usually used in combined heat and power plant. For water with a temperature below 100 ºC, binary (Organic Rankine Cycle) power plants are usually used to generate electricity. Besides this technology, the thermoelectric generator (TEG) technology is considered as a new way to produce

power for low-temperature geothermal resources (Li *et al.*, 2013). Comparing with the conventional methods of generating electricity from geothermal energy using ORC technology, the thermoelectric method can directly convert heat into electricity by Seebeck effect.and has numerous advantages, including direct energy conversion, no moving parts and no working fluids inside the thermoelectric generator, no maintenance and no extra costs, no land needed, superior scalability, long lifespan, independent of the hour of the day and season, noiseless operations, high reliability and environmental friend. In addition, it has a wider choice of thermal sources. It can utilize both the high- and low-quality heat to generate power while the ORC technology works ineffectively for the low-quality heat (Champier, 2017, Chet *et al.*, 2015, Date *et al.*, 2014, Ding *et al.*, 2017, Hsiao *et al.*, 2010, Li *et al.*, 2013).

The aim of this work is to find an alternative method in which electric power may be generated in downhole with thermoelectric technology and coaxial borehole heat exchanger technology in geothermal wells, which is different from traditional ORC or Kalina technology. The coaxial borehole heat exchanger recovers heat from surrounding formation, and transfers the heat to thermoelectric modules to generate power in downhole. Mathematical models are developed to study the downhole temperature distributions related to the power generation. Then, a case study with cost-benefit analysis will be conducted to validate the potential of downhole thermoelectric power generation in geothermal wells under different carbon taxes.

2. SYSTEM DESIGN OF DOWNHOLE THERMOELECTRIC POWER GENERATION SYSTEM WITH COAXIAL BOREHOLE HEAT EXCHANGER

A thermoelectric generator (TEG) is a device that directly converts a heat gradient into electricity through the Seebeck effect, which is the phenomenon that electric current induced by temperature difference in an electrical conductor. A TEG is usually made up of ceramic substrates, electrical insulators, electrical conductors, and many N-type and P-type semiconductors with high Seebeck coeffcients which are alternately connected in series electrically and in parallel thermally as showed in Figure 1. Recently, power generation with thermoelectric technology has been proposed to harvest and utilize geothermal energy in downhole (Liu *et al.*, 2017a, Liu *et al.*, 2017b, Liu *et al.*, 2017c, Liu *et al.*, 2020, Wang *et al.*, 2018). Combining with a coaxial borehole heat exchanger, a new design of downhole thermoelectric power generation in geothermal wells is presented (Figure 2).

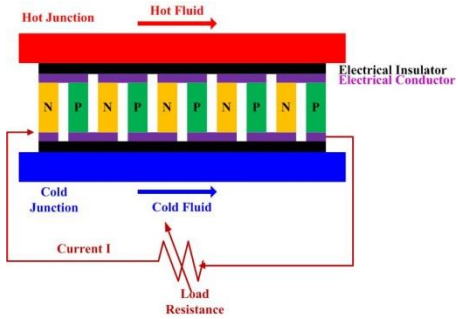

Figure 1: Schematic of a thermoelectric generator

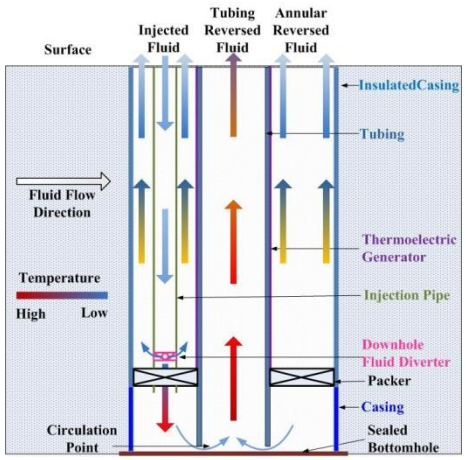

Figure 2: Schematic of downhole thermoelectric power generation design with a coaxial borehole heat exchanger in a geothermal well

In the proposed design, the well bottom is sealed completely and the casing is lowered to well bottom to prevent leakage between formation and borehole. Tubing is run into casing and downed to right above of the sealed bottom. A packer will be set at the top of production zone to isolate the casing-tubing annulus. An injection pipe assembled with a downhole fluid diverter will be run into the casing-tubing annulus and just pass through the packer. The downhole fluid diverter is just located above the packer and is used to adjust fluid flowing into the casing-tubing annulus above and below the packer. The outer surfaces of the tubing above the packer are fully covered with thermoelectric modules. Cold fluid will be continuously injected downwards in the injection pipe from the surface. When the cold fluid flows pass the downhole fluid diverter, part of the cold fluid will be diverted and enters into the casing-tubing annulus above the packer; the other part will continuously flow downwards through the packer and enters into the casing-tubing annulus below the packer, which will reverse back at the circulation point due to the sealed bottomhole. The diverted cold fluid at downhole fluid diverter flows upwards along the casing-tubing annulus above the packer and provides cold sources for

TEGs. While the other part of the cold fluid continuously flows downwards along the casing-tubing annulus below the packer, it adsorbs heat from the surrounding formation gradually and becomes high-temperature fluid at the bottom of the well. At the circulation point, the heated fluid flows upwards in tubing to the surface and provides heat sources for TEGs. At the same well depth, the temperature of upward flowing fluid in tubing is higher than that of upward flowing fluid in casing-tubing annulus. Once the system achieves a stable temperature difference between tubing and casing-tubing annulus by continuously injecting and circulating the cold fluid, electricity will be generated as the response to applied temperature gradient and the produced electricity could be transmitted to surface and input to local grid. In general, the proposed design includes two sections, one is the heat harvesting section located below the packer, which harvests heat from surrounding hot formation with coaxial borehole heat exchanger; and the other is thermoelectric power generation section located above the packer, which produces power by temperature difference across both sides of TEGs.

In order to create a temperature as larger as possible across both sides of TEGs, the upper casing above the packer are coated with insulation materials to reduce heat transferring from the surrounding formation to the fluid flowing in casing-tubing annulus, while the lower casing below the packer has a good heat conductivity to harvest enough geothermal energy from deeper formation to heat the injected cold fluid in it. Tubing surface are also coated with thermal insulation materials and the injection pipe will be insulted completely.

3. MATHEMATICL MODEL

3.1 Downhole Temperature Model

To assess the performance of the proposed downhole power generation design, it is necessary to know the temperature distributions along the tubing, the casing-tubing annulus and both sides of TEGs. The assumptions are made: (1) Injection pipe is perfectly insulated; the packer length and the injection pipe length which extending out of the packer are ignored, that is the inlet temperatures of the injected cold fluid at the casing-tubing annulus above the packer and below the packer are the same as the inlet temperature at surface; 2) The heat transfer between formation and wellbore is in steady state; 3) Temperature drop across both tubing and casing walls are neglected due to high thermal conductivity of metals as well as the small thickness of the walls; 4) Thermoelectric elements in TEG are identical and their geometric configurations are in the optimum form; 5)External heat-transfer irreversibilities between the thermoelectric devices and the heat reservoirs are neglected; 6) Seebeck coefficient, thermal conductance, electrical resistance, and figure of merit of the thermoelectric devices are independent of temperature in the range of studied temperatures;7) Fluid in tubular flows in one-dimension axial direction and heat conducts in one-dimension radical direction.

Heat exchanges among tubing fluid, casing-tubing annular fluid, coaxial borehole heat exchanger and surrounding formation result in temperature difference on both sides of TEGs. To obtain temperature distributions in casing-tubing annulus, tubing and coaxial borehole heat exchanger, an heat balance over an element of length, dz, which is treated as a control volume at distance of dz from the surface where *z* equals to zero, was built. Here z is positive in the downward direction. The schematic of heat balance for tubular and formation is shown in Figure 3.

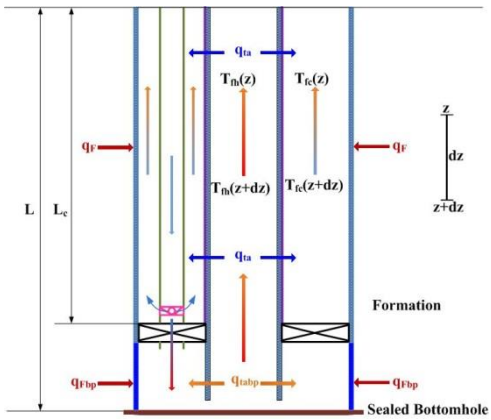

Figure 3: Schematic of heat balance for tubular and formation

3.1.1 Below Packer (Heat Harvesting Section)

The flow conduits below the packer work as a coaxial borehole heat exchanger. In the casing-tubing annulus below the packer, the injected fluid is in direct contact with casing inner wall. In the tubing, the reversed fluid from the circulation point flows up and enters into thermoelectric power generation section, the heat transfer occurs only through the tubing wall (Alimonti & Soldo, 2016, Kabir *et al.*, 1996, Willhite, 1967). In this study, water was selected as the working fluid. For the fluid flows from depth of z to $(z + dz)$ in casing-tubing annulus and from depth of $(z + dz)$ to z in tubing below the packer, energy balance equations could be established accordingly.

$$q_{fhbp}(z + dz) = q_{fhbp}(z) + q_{tabp} \quad (1)$$

$$q_{fcbp}(z + dz) = q_{fcbp}(z) + q_{tabp} + q_{Fbp} \quad (2)$$

Where, q_{fhbp} is the heat of the reversed fluid in tubing below the packer, J; q_{fcbp} the heat of the injected fluid in casing-tubing annulus below the packer, J; q_{tabp} is the heat flow from the tubing to the casing-tubing annulus, J; q_{Fbp} is the heat flow from the surrounding formation to the casing-tubing annulus, J.

Based on the heat transfer theory, the heat balance for fluid flowing in the tubing and in the casing-tubing annulus below the packer are respectively given by:

$$q_{fhbp}(z+dz) - q_{fhbp}(z) = c_w w_{injbp}\left[T_{fhbp}(z+dz) - T_{fhbp}(z)\right] \tag{3}$$

$$q_{fcbp}(z+dz) - q_{fcbp}(z) = c_w w_{injbp}\left[T_{fcbp}(z+dz) - T_{fcbp}(z)\right] \tag{4}$$

Where, c_w is the water specific heat capacity, J/(kg.K); w_{injbp} is the mass of the injected fluid in the casing-tubing annulus below the packer, kg; T_{fhbp} is the fluid temperature in the tubing below the packer, K; T_{fcbp} is the fluid temperature in the casing-tubing annulus below the packer, K.

Heat flow, q_{Fbp}, from surrounding formation to casing-tubing annulus below the packer is given by,

$$q_{Fbp} = 2\pi r_c U_{abp}\left(T_{wb}(z) - T_{fcbp}(z)\right)dz \tag{5}$$

Heat flow, q_{ta}, from tubing to casing-tubing annulus below the packer is given by,

$$q_{tabp} = 2\pi r_t U_{tbp}\left(T_{fhbp}(z) - T_{fcbp}(z)\right)dz \tag{6}$$

Where, r_c is the casing radius, m; r_t is the tubing radius, m; T_{wb} is the temperature at wellbore/formation interface, K; U_{abp} is the overall heat transfer coefficient of casing-tubing annulus below the packer, which depends on the resistances to heat flow through casing-tubing annular fluid, casing metal and cement, W/(m.K); U_{tbp} is the overall heat transfer coefficient of tubing blow the packer, which depends on the resistances to heat flow through the tubing fluid and tubing metal, W/(m.K). U_{abp} and U_{tbp} can be calculated by the many methods(Edwardson *et al.*, 1962, Hasan & Kabir, 2002).

Assuming that the temperature at wellbore/formation interface along the vertical direction changes linearly, that is:

$$T_{wb} = T_{surface} + g_G z \tag{7}$$

Where, $T_{surface}$ is the surface temperature of the wellbore/formation interface, K; g_G is the geothermal gradient, K/m; z is the well depth from surface, m.

Letting,

$$A = \frac{c_w w_{injbp}}{2\pi r_c U_a} \qquad B = \frac{c_w w_{injbp}}{2\pi r_t U_t}$$

Simplifying these equations based on the assumptions of incompressible, single-phase fluid, and the following equations can be obtained,

$$A\frac{dT_{fcbp}}{dz} = \left(T_{wb} - T_{fcbp}\right) - \frac{A}{B}\left(T_{fcbp} - T_{fhbp}\right) \tag{8}$$

$$\frac{dT_{fhbp}}{dz} = \frac{T_{fhbp} - T_{fcbp}}{B} \tag{9}$$

The boundary conditions could be found that the temperature of the reversed fluid at tubing inlet is equal to the temperature of the injected fluid in casing-tubing annulus at the circulation point, and the temperature of the injected fluid at the outlet of injection pipe is known. Here, we assume that the depth of the tubing inlet (circulation point) is the same as the well bottom.

at the tubing inlet(circulation point): $z = \mathrm{L}$ $T_{fhbp} = T_{fcbp}$ (10)

at the injection pipe outlet : $z = L_c$ $T_{fcbp} = T_{inj}$ (11)

Where, L is the depth of the tubing inlet or the circulation point or the well bottom, m; L_c is the depth of cold fluid entering into the casing-tubing annulus below the packer or the depth of the downhole fluid diverter or the depth of injection pipe outlet, m; T_{inj} is the temperature of injected liquid at the surface, K.

Applying boundary conditions, the temperature distribution along tubing and casing-tubing annulus can be solved and expressed as,

$$T_{fhbp}(z) = me^{\lambda_1 z} + ne^{\lambda_2 z} + T_{surface} + g_G z + Bg_G + T_{wb}(L_c) \tag{12}$$

$$T_{fcbp}(z) = (1-\lambda_1 B)me^{\lambda_1 z} + (1-\lambda_2 B)ne^{\lambda_2 z} + T_{wb}(L_c) + T_{surface} + g_G z \tag{13}$$

Where, $T_{wb}(L_c)$ is the formation temperature at the packer, K.

In Eqs.12 and 13, λ_1, λ_2, m and n are all constants, given as follows.

$$\lambda_1 = -\frac{1}{2A} + \frac{1}{2A}\sqrt{1+\frac{4A}{B}}$$

$$\lambda_2 = -\frac{1}{2A} - \frac{1}{2A}\sqrt{1+\frac{4A}{B}}$$

$$m = -\frac{\left(T_{inj} - T_{wb}(L_c)\right)\lambda_2 e^{\lambda_2(L-L_c)} + g_G(1-\lambda_2 B)}{\lambda_1 e^{\lambda_1(L-L_c)}(1-\lambda_2 B) - \lambda_2 e^{\lambda_2(L-L_c)}(1-\lambda_1 B)}$$

$$n = \frac{\left(T_{inj} - T_{wb}(L_c)\right)\lambda_1 e^{\lambda_1(L-L_c)} + g_G(1-\lambda_1 B)}{\lambda_1 e^{\lambda_1(L-L_c)}(1-\lambda_2 B) - \lambda_2 e^{\lambda_2(L-L_c)}(1-\lambda_1 B)}$$

3.1.2 Above Packer (Power Generation Section)

For the fluid heated in casing-tubing annulus below the packer and flowing upward in the tubing, it enters at the depth of (z + dz) and leaves at z with heat convection towards casing-tubing annulus above the packer; and for the fluid flowing upward in the casing-tubing annulus above the packer, the energy balance involves heat transfer from tubing to casing-tubing annulus above the packer and heat transfer from surrounding formation(Kabir *et al.*, 1996, Willhite, 1967). Following the same steps as indicated in section 3.1.1, the temperature distributions along tubing and casing-tubing annulus can be solved and expressed as,

$$T_{fh}(z) = me^{\lambda_1 z} + ne^{\lambda_2 z} + T_{surface} + g_G(z+\xi) \tag{14}$$

$$T_{fc}(z) = (1-\lambda_1 B)me^{\lambda_1 z} + (1-\lambda_2 B)ne^{\lambda_2 z} + T_{surface} + g_G(z+\xi-B) \tag{15}$$

Where, T_{fh} is the fluid temperature in the tubing above the packer, K; T_{fc} is the fluid temperature in the casing-tubing annulus above the packer, K.

In Eqs.14 and Eqs.15, ξ, λ_1, λ_2, m and n are all constants, given as follows.

$$C = \frac{c_w w_{inj}}{2\pi r_c U_a} \qquad D = \frac{c_w w_t}{2\pi r_t U_t} \qquad E = \frac{c_w w_{inj}}{2\pi r_t U_t}$$

$$\xi = \frac{CD + DE + CE}{E}$$

$$\lambda_1 = \frac{CD + DE + CE + \sqrt{(CD+DE+CE)^2 - 4CDE^2}}{2CDE}$$

$$\lambda_2 = \frac{CD + DE + CE - \sqrt{(CD+DE+CE)^2 - 4CDE^2}}{2CDE}$$

$$m = \frac{(1-\lambda_2 D)\times\left(T_{fhbp}(L_c) - T_{surface} - g_G(L_C+\xi)\right) - (T_{inj} - T_{surface} - g_G(L_C+\xi-D))}{D\times(\lambda_1-\lambda_2)e^{\lambda_1 L_C}}$$

$$n = \frac{(1-\lambda_1 D)\times\left(T_{fhbp}(L_c) - T_{surface} - g_G(L_C+\xi)\right) - (T_{inj} - T_{surface} - g_G(L_C+\xi-D))}{D\times(\lambda_2-\lambda_1)e^{\lambda_2 L_C}}$$

3.2 Electrical Power Generation

The thermoelectric modules are attached on the outer surface of the tubing tightly and their geometric configurations are in the optimum state. When the flowing temperature in tubing and casing-tubing annulus are known, then the temperature on the hot and cold surfaces of TEGs can be deduced from heat transfer theory (Suzuki & Tanaka, 2003) and expressed as following.

$$T_{mh} = T_{fh} - \frac{2\pi r_{pn} U_t}{h_t}\left(T_{fh} - T_{fc}\right) \tag{16}$$

$$T_{mc} = T_{fc} + \frac{2\pi r_{pn} U_t}{h_c}\left(T_{fh} - T_{fc}\right) \tag{17}$$

Where, T_{mh} is the temperature on the hot surface of TEG, K; T_{mc} is the temperature on the cold surface of TEG, K; r_{pn} is the radius after the thermoelectric modules are attached on the external surface of the tubing, m; h_t is the convective heat transfer coefficient between the produced fluid and the tube, W/(m.K); h_c is the convective heat transfer coefficient between the injected fluid and the case, W/(m.K).

According to the principle of the TEG, the produced voltage depends on the temperature difference and Seebeck coefficient (Chen *et al.*, 2010, Gou *et al.*, 2013, Reddy *et al.*, 2013). For an element of length (dz), the temperature along each side of TEG keeps constant. Then the total voltage, E, can be integrated along the wellbore and are given by,

$$E = \int_0^L \alpha(T_{mh} - T_{mc})dz = n_\phi n_x \alpha \int_0^L \big(T_{mh}(z) - T_{mc}(z)\big)dz \tag{18}$$

Where, e is the voltage of a thermoelectric element, V; n_ϕ and n_x are the number of thermoelectric pairs in a circumferential circulation and the number density of thermoelectric pairs in the axial direction, respectively, dimensionless.

When the thermoelectric module is applied a certain temperature gradient, electric power is produced and it is defined as,

$$P = \frac{E^2}{2R + R_L + \frac{R^2}{R_L}} \tag{19}$$

Where, P is the output power, W; R is the internal electric resistance of TEG, Ω; R_L is the external electric resistance, Ω.

By considering the Seebeck effect, the thermal power input to the hot side in *ith* segment, Q_{Hi}, and the thermal power output from the cold side of in *ith* segment, Q_{Ci}, are separately given by(Kim, 2013, Lineykin & Ben-Yaakov, 2007),

$$Q_{Hi} = K\big(T_{mh(i)} - T_{mc(i)}\big) + \alpha T_{mh(i)} I - \frac{1}{2} I^2 R \tag{20}$$

$$Q_{ci} = K\big(T_{mh(i)} - T_{mc(i)}\big) + \alpha T_{mc(i)} I + \frac{1}{2} I^2 R \tag{21}$$

Where, K is the thermal conductance of TEG, W/(m.K).

The efficiency of TEG can be defined as,

$$\eta = \frac{P_t}{\sum Q_{Hi}} \tag{22}$$

Where, P_t is the total output power, W.

3.3 Required Pumping Power

In our proposed design, a surface pump is used to inject and circulate the cold fluid in injection pipe, casing-tubing annulus, coaxial borehole heat exchanger and tubing. To attain the required pumping power, the pressure losses in injection pipe, casing-tubing annulus, coaxial borehole heat exchanger and tubing should be determined. According to single phase flow theory, the required pumping power can be obtained.

$$P_{pump} = Q_{inj}\big[\Delta P_{dip} + \omega \Delta P_{ua} + (1-\omega)(\Delta P_{ut} + \Delta P_{dc} + \Delta P_{uc})\big] \tag{23}$$

Where, P_{pump} is the required pumping power, W; Q_{inj} is the injection rate at surface, m^3/s; ΔP_{dc} is the pressure loss in downward coaxial borehole heat exchanger (casing-tubing annulus below the packer), Pa; ΔP_{uc} is the pressure losses in upward coaxial borehole heat exchanger (tubing below the packer), Pa; ω is the ratio of the flow rate entering into casing-tubing annulus above the packer to the total injection rate.

Assuming the pumping power is supplied by the produced power from the same well, then the net power is given by,

$$P_{net} = P_t - P_{pump} \tag{24}$$

Where, P_{net} is the net power, W.

3.4 Cost-benefit Assessment

A cost-benefit assessment was performed to evaluate the economic feasibility of downhole thermoelectric power generation in a geothermal well. Here, we assume that the geothermal well has already existed, what we only need to do is to retrofit the well suitable for power generation. Therefore, only the capital cost of the TEG system installation and the circuitry construction are considered in the cost-benefit assessment. In addition, the power generation by geothermal energy has a large environment benefit. More than 90% of greenhouse gas emissions could be reduced if the electrical energy produced from a fossil fuel power plant is replaced by geothermal energy(Glassley, 2010). Therefore, the carbon tax income is included in the cost-benefit assessment.

4. RESULTS AND DISCUSSION

4.1 Parameters for case studies

In this case study, downhole thermoelectric power generation system will be applied in a liquid dominated geothermal well.. The top depth of the production zone in the geothermal well is 3000 m and the thickness of the production zone is 500m. It was completed with 9-5/8'' casing to the bottom. A packer was set right above the production zone with 3-1/2'' tubing connected to surface. As designed, an injection pipe with inner diameter of 1-5/8'' is run through the casing-tubing annulus down to the depth of

3000 m and just penetrating the packcer. The daily injection rate is 500 m^3 and the fluid diversion ratio between the fluid entering into casing-tubing annulus above the packer and below the packer is 1. The casing above the packer is coated with an insulation material with thermal conductivity of 0.06 W/(m•K), while the casing below the packer is highly heat conductivity with thermal conductivity of 43.25 W/(m•K) and is good cemented with formation. The tubing is also coated with an insulation material with thermal conductivity of 0.06 W/(m•K) while the injection pipe is perfect insulated. The injected fluid will reversely flow upwards in tubing at 3500m. Segmented thermometric generators are connected in series and fully mounted on the outer surface of tubing above the packer. Data used in this study are summarized in Table 1.

Table 1 Parameters for case study of downhole thermoelectric power generation

Parameters	Value
Tubing outer diameter(m)	0.089
Tubing inner diameter(m)	0.076
Casing outer diameter(m)	0.244
Casing inner diameter(m)	0.224
Injection pipe outer diameter(m)	0.041
Injection pipe inner diameter(m)	0.035
Wellbore depth(m)	3500
Packer depth(m)	3000
Coaxial heat exchanger length(m)	500
Geothermal gradient(°C/m)	0.035
Surface temperature(°C)	21
Reservoir temperature(°C)	126
Cold fluid injection temperature(°C)	20
Cold fluid injection rate(m^3/d)	500
Fluid diversion ratio(/)	1
Water specific heat capacity(kJ/ (kg•K))	4.18
Thermal conductivity of formation(W/(m•K))	2.42
Thermal conductivity of insulation material(W/(m•K))	0.06
Thermal conductivity of casing(W/(m•K))	43.25

For downhole thermoelectric modules, Bi_2Te_3-based materials are selected as the semiconductor due to its commercially availability, high performance and proven engineering applications (Chet *et al.*, 2015). TEG parameters are shown in Table 2. The length of each segment of TEG is assumed to be same as the tubing length for convenient assembling and running into downhole.

Table 2 Thermoelectric properties and parameters in this case study

Parameters		Value
P-type: $Bi_{2-x}Sb_xTe_3$	Seebeck coefficient(μV/K)	222.48
	Electrical resistivity(μΩ•m)	12.5
	Thermal conductivity(W/(m•K))	1.36
	Length(m)	0.013
	Cross-section area(cm^2)	0.25
N-type: $Bi_2Se_{3-y}Te_y$	Seebeck coefficient(μV/K)	-223.06
	Electrical resistivity(μΩ•m)	12.9
	Thermal conductivity(W/(m•K))	1.41
	Length(m)	0.013
	Cross-section area(cm^2)	0.25

4.2 Results for case studies

4.2.1 Temperature distribution

Temperature distribution in tubing, casing-tubing annulus, hot and cold sides of TEG are presented in Fig.4. As the fluid diverted from the downhole fluid diverter flows through the packer and enters into the casing-tubing annulus, it is heated to about 123.5°C at the well bottom. While it reverses and flows upwards in tubing, it releases heat to the "cold" fluid in casing-tubing annulus below the packer and the temperature of the reversed fluid at packer drops to 120.1°C. When the heated fluid continuously flows upwards in tubing, some heats are transferred to TEG and the reversed fluid in casing-tubing annulus above the packer, the wellhead temperature of the reversed fluid in tubing is high up to 97.0°C, which is hot enough to be further used on the ground.

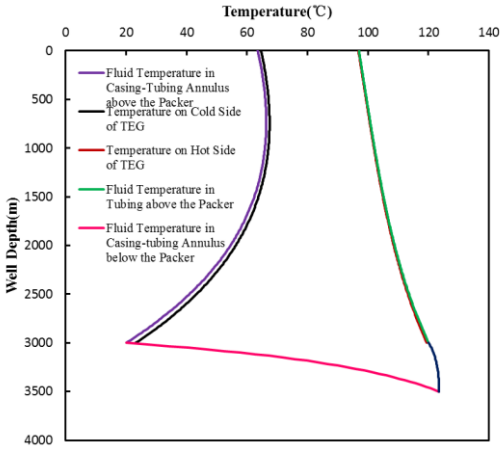

Figure 4: Temperature distributions in tubing, casing-tubing annulus and both sides of TEG

As the fluid flows upwards in casing-tubing annulus above the packer, it is heated up by 43.5°C due to heat conducting from surrounding formation and transferring from TEG and tubing. The temperature differences among the reversed fluid in tubing and the hot side of TEG, the reversed fluid in casing-tubing annulus and the cold side of TEG are relatively small. However, the temperature differences across both sides of TEG vary from 96.3°C at the packer to 32.2°C at the wellhead. Such temperature differences are large enough to produce electric power(Liu, 2014). The continuous injected cold fluid not only maintains a lower temperature environment in the cold side of thermoelectric module, but also provides heated fluid for direct use on the ground.

4.2.2 Power generation

In this study, the net electric power from a single geothermal well is up to 228.06kW with the proposed design. The power capacity is some smaller in a single well, but a scale benefit will be achieved when a cluster of geothermal wells are included and the reversed fluids from tubing are sent to binary power plant as a complementary. Thermoelectric performances are listed in Table 3.

Table 3 Thermoelectric Performances in this case study

Parameters	Value
Figure of merit (1/K)	0.0028
Dimensionless figure of merit (/)	0.901
Total produced power (kW)	320.56
Required pumping power (kW)	92.50
Net electric power (kW)	228.06
Thermal to electricity conversion efficiency(%)	6.63

4.2.3 Economical evaluation

As the previous discussion, only the capital cost of TEG system installation and circuitry construction are considered in this study. According to the dimensions of P-N type semiconductors and the length and diameter of tubing, total 126,000 thermoelectric modules (each module is made up of 16×16 P-N type semiconductors) are needed to be mounted on the outer surface of tubing. Assuming the cost of a thermoelectric module is 35 RMB, the costs of accessories and installations are 25% of the total cost of thermoelectric modules(Chen *et al.*, 2013). The cost parameters are listed in Table 4.

Table 4 Capital cost of a downhole thermoelectric power generation system

Parameters	per Price (RMB)	Quantity	Total Cost ($\times 10^4$RMB)
Thermoelectric module	35	126,000	441
Voltage regulator system	2,500	20	5

Electric storage system	/	/	200
Accessories and installations	/	/	110.25
Total capital cost			756.25

Electricity generation from geothermal resources results in much lower greenhouse gas (GHG) emissions than that from traditional fossil fuels(Noorollahi & Itoi, 2011). According to the report by National Renewable Energy Laboratory (NREL), the median life cycle GHG emissions from enhanced geothermal systems binary, hydrothermal flash, and hydrothermal binary plants were found to be 32 g CO_2 eq/kWh, 47 g CO_2 eq/kWh and 11.3 g CO_2 eq/kWh respectively (Eberle *et al.*, 2017). For power generation from coal-fired plant, the median life cycle GHG emission is estimated to be 1018 g CO_2 eq/kWh(Jiang *et al.*, 2013). If the average median life cycle GHG emission from geothermal resources is taken as 30 g CO_2 eq/kWh, the reduction of GHG emissions is 988 g CO_2 eq/kWh when the electricity generated from a coal-fired plant is replaced by a geothermal power plant. It is assumed that carbon tax will be imposed on power plant in the future. Supposing carbon tax is 20 ~ 200 RMB/t CO_2 (Jiang *et al.*, 2013), then an additional income of a geothermal power plant will increase 0.0198~0.1976 RMB/ kWh. The parameters used for cost-benefit analysis are shown in Table 5 and the results for different carbon tax scenarios are presented in Table 6.

Table 5 Parameters used for cost-benefit analysis

Parameters	Value
Electric price(RMB/kWh)	1
Operation life(Year)	18
Annual operation time(Hours)	6000
Fixed depreciation period(Year)	10
Income tax(%)	25
Benchmark return on investment(%)	9
Base rate of return(%)	6
Discount rate(%)	6

Table 6 Results of cost-benefit analysis for different carbon tax scenarios

Parameters	Carbon Tax(RMB/t CO_2)		
	0	20	200
Annual net income(10^4RMB)	121.53	123.57	141.81
Rate of return(%)	16.07	16.34	18.75
Static payback period(Year)	6.22	6.12	5.33
Dynamic payback period (Year)	8.02	7.85	6.62
Net present value(10^4RMB)	559.66	581.67	779.24

It can be seen that the investment could be returned in 6 to 8 years and the rate of return is larger than 16% for different carbon tax scenarios. Based on above calculation, the downhole thermoelectric power generation with coaxial borehole heat exchanger is feasible and economically competitive.

5. CONCLUSIONS

(1) Downhole thermoelectric power generation with a coaxial borehole heat exchanger in geothermal wells is a new way to utilize geothermal energy in downhole without affecting subsequent utilization on the ground. In a geothermal well with the depth of 3500m including 500m length of heat exchanging zone, the net power output of 228.06 kW and thermal-to-electricity conversion efficiency of 6.63% are obtained. The payback period under different carbon tax scenarios is about 6 – 8 year and the rate of return is larger than 16%.

(2) Injection rate and fluid diversion ratio will influence the produced power, required pumping power and thermal-to-electricity conversion efficiency. Larger flow rate will accelerate the heat transfer process and keep a larger temperature difference across both sides of TEG. The reasonable power and efficiency will be obtained with injection rate of 600m^3/d and fluid diversion ratio of 1.5 – 2.0.

(3) Higher temperature difference is crucial for better downhole thermoelectric performance. Proposed downhole thermoelectric power generation design with coaxial borehole heat exchanger is also applicable for abandoned geothermal wells, enhanced geothermal systems, and abandoned oil and gas wells.

Reference

Alimonti, C., Berardi, D., Bocchetti, D. & Soldo, E. (2016). Coupling of energy conversion systems and wellbore heat exchanger in a depleted oil well. *Geothermal Energy* **4**.

Alimonti, C. & Soldo, E. (2016). Study of geothermal power generation from a very deep oil well with a wellbore heat exchanger. *Renewable Energy* **86**, 292-301.

Bertani, R. (2016). Geothermal power generation in the world 2010-2014 update report. *Geothermics* **60**, 31-43.

Champier, D. (2017). Thermoelectric generators: A review of applications. *Energy Conversion and Management* **140**, 167-181.

Chen, H. P., Yu, X. W., Shi, Z. Y., Wang, Z. P. & Wu, W. H. (2013). Experimental study and economical analysis of a geothermal electric power generation system. *Electric Power Science and Engineering* **29**, 63-67.

Chen, M., Lund, H., Rosendahl, L. A. & Condra, T. J. (2010). Energy efficiency analysis and impact evaluation of the application of thermoelectric power cycle to today's CHP systems. *Applied Energy* **87**, 1231-1238.

Chet, D. L., Singh, B., Remeli, M. F., Date, A., Singh, R. & Akbarzadeh, A. (2015). Prospects of Power Generation from Geothermal Energy Using Thermoelectric Modules. *World Geothermal Congress 2015*. Melbourne, Australia.

Date, A., Date, A., Dixon, C. & Akbarzadeh, A. (2014). Progress of thermoelectric power generation systems: Prospect for small to medium scale power generation. *Renewable & Sustainable Energy Reviews* **33**, 371-381.

Ding, L. C., Meyerheinrich, N., Tan, L., Rahaoui, K., Jain, R. & Akbarzadeh, A. (2017). Thermoelectric power generation from waste heat of natural gas water heater. *Energy Procedia* **110**, 32-37.

DiPippo, R. (2008). *Geothermal Power Plants: Princi Applications, Case Studies and Environmental Impact (Second Edition)*. The Netherlands, The Boulevard, Langford Lane, Kidlington, OX5 1GB, Oxford, UK.: Elsevier Science.

Eberle, A., Heath, G., Nicholson, S. & Carpenter, A. (2017). Systematic Review of Life Cycle Greenhouse Gas Emissions from Geothermal Electricity. Technical Report, National Renewable Energy Laboratory.

Edwardson, M. J., Girner, H. M., Parkison, H. R., Williams, C. D. & Matthews, C. S. (1962). Calculation of formation temperature disturbances caused by mud circulation. *Journal of Petroleum Technology* **14**, 416-426.

Feng, Y., Tyagi, M. & White, C. D. (2015). A downhole heat exchanger for horizontal wells in low-enthalpy geopressured geothermal brine reservoirs. *Geothermics* **53**, 368-378.

Gando, A., Gando, Y., Ichimura, K., Ikeda, H., Inoue, K., Kibe, Y., Kishimoto, Y., Koga, M., Minekawa, Y., Mitsui, T., Morikawa, T., Nagai, N., Nakajima, K., Nakamura, K., Narita, K., Shimizu, I., Shimizu, Y., Shirai, J., Suekane, F., Suzuki, A., Takahashi, H., Takahashi, N., Takemoto, Y., Tamae, K., Watanabe, H., Xu, B. D., Yabumoto, H., Yoshida, H., Yoshida, S., Enomoto, S., Kozlov, A., Murayama, H., Grant, C., Keefer, G., Piepke, A., Banks, T. I., Bloxham, T., Detwiler, J. A., Freedman, S. J., Fujikawa, B. K., Han, K., Kadel, R., O'Donnell, T., Steiner, H. M., Dwyer, D. A., McKeown, R. D., Zhang, C., Berger, B. E., Lane, C. E., Maricic, J., Miletic, T., Batygov, M., Learned, J. G., Matsuno, S., Sakai, M., Horton-Smith, G. A., Downum, K. E., Gratta, G., Tolich, K., Efremenko, Y., Perevozchikov, O., Karwowski, H. J., Markoff, D. M., Tornow, W., Heeger, K. M., Decowski, M. P. & Collaboration, K. (2011). Partial radiogenic heat model for Earth revealed by geoneutrino measurements. *Nature Geoscience* **4**, 647-651.

Glassley, W. E. (2010). *Geothermal energy: renewable energy and the environment*. Boca Raton, Florida, USA: CRC Press. Taylor & Francis Group.

Goldstein, B., Hiriart, G., Bertani, R., Bromley, C., Gutierrez-Negrin, L., Huenges, E., Muraoka, H., Ragnarsson, A., Tester, J. & Zui, J. (2011). Geothermal Energy. In: Edenhofer, O., Pichs-Madruga, R., Sokona, Y., Seyboth, K., Matschoss, P., Kadner, S., Zwickel, T., Eickemeier, P., Hansen, G., Schlomer, S. & von Stechow, C. (eds.) *IPCC Special Report on Renewable Energy Sources and Climate Change Mitigation*. Cambridge, United Kingdom.

Gou, X. L., Yang, S. W., Xiao, H. & Ou, Q. (2013). A dynamic model for thermoelectric generator applied in waste heat recovery. *Energy* **52**, 201-209.

Hasan, A. R. & Kabir, C. S. (2002). *Fluid Flow and Heat Transfer in Wellbores*: Society of Petroleum Engineers.

Hsiao, Y. Y., Chang, W. C. & Chen, S. L. (2010). A mathematic model of thermoelectric module with applications on waste heat recovery from automobile engine. *Energy* **35**, 1447-1454.

IRENA. (2021). Renewable energy highlights. Masdar City,Abu Dhabi,United Arab Emirates: International Renewable Energy Agency.

Jiang, J., Ye, B. & Ma, X. (2013). The Impact of International Greenhouse Gas Emission Constraints on Coal-Fired Power Plant in China-Based on LCAModel. *IEEE Computer Society* **415**, 1468-1472.

Kabir, C. S., Hasan, A. R., Kouba, G. E. & Ameen, M. (1996). Determining Circulating Fluid Temperature in Drilling, Workover, and Well Control Operations. *SPE Drilling & Completion* **11**, 74-79.

Kim, S. (2013). Analysis and modeling of effective temperature differences and electrical parameters of thermoelectric generators. *Applied Energy* **102**, 1458-1463.

Li, K. W., Liu, C. W. & Chen, P. Y. (2013). Direct power generation from heat without mechanical work. *Thirty-Eighth Workshop on Geothermal Reservoir Engineering*. Stanford University,Stanford, California.

Lineykin, S. & Ben-Yaakov, S. (2007). Modeling and analysis thermoelectric modules. *IEEE Transactions on Industry Applications* **43**, 505-512.

Liu, J. R., Du, P., Li, B. Y., Shi, W. X. & Cao, S. J. (2017a). The cold source type hot dry rock formation thermoelectric power generation system and method. In: Administration, C. N. I. P. (ed.). China.

Liu, J. R., Du, P., Li, B. Y., Shi, W. X. & Cao, S. J. (2017b). The external source type hot dry rock formation thermoelectric power generation system and method. In: Administration, C. N. I. P. (ed.). China.

Liu, J. R., Li, B. Y., Y., L. D., Wang, Y. Y., Du, P., Shi, W. X. & Cao, S. J. (2017c). Compound cold source hot dry rock thermoelectric power generation system and method. In: Administration, C. N. I. P. (ed.). China.

Liu, J. R., Wang, Z., Shi, K. Y., Li, Y. Q., Liu, L. X. & Wu, X. R. (2020). Analysis and modeling of thermoelectric power generation in oil wells: A potential power supply for downhole instruments using in-situ geothermal energy. *Renewable Energy* **150**, 561-569.

Liu, L. P. (2014). Feasibility of large-scale power plants based on thermoelectric effects. *New Journal of Physics* **16**.

Lund, J. W. (2003). The use of downhole heat exchangers. *Geothermics* **32**, 535-543.

Morita, K., Tago, M. & Ehara, S. (2005). Case Studies on Small-Scale Power Generation with the Downhole Coaxial Heat Exchanger. *World Geothermal Congress 2005*. Antalya, Turkey.

Nalla, G., Shook, G. M., Mines, G. L. & Bloomfield, K. (2004). Parametric sensitivity study of operating and design variables in wellbore heat exchangers. *Workshop on geothermal reservoir engineering*. Stanford University,Stanford, California.

Noorollahi, Y., Bina, S. M. & Yousefi, H. (2016). Simulation of Power Production from Dry Geothermal Well Using Down-hole Heat Exchanger in Sabalan Field, Northwest Iran. *Natural Resources Research* **25**, 227-239.

Noorollahi, Y. & Itoi, R. (2011). Production capacity estimation by reservoir numerical simulation of northwest (NW) Sabalan geothermal field, Iran. *Energy* **36**, 4552-4569.

Reddy, B. V. K., Barry, M., Li, J. & Chyu, M. K. (2013). Mathematical modeling and numerical characterization of composite thermoelectric devices. *International Journal of Thermal Sciences* **67**, 53-63.

Suzuki, R. O. & Tanaka, D. (2003). Mathematic simulation on thermoelectric power generation with cylindrical multi-tubes. *Journal of Power Sources* **124**, 293-298.

Tomasini-Montenegro, C., Santoyo-Castelazo, E., Gujba, H., Romero, R. J. & Santoyo, E. (2017). Life cycle assessment of geothermal power generation technologies: An updated review. *Applied Thermal Engineering* **114**, 1119-1136.

Wang, K., Liu, J. R. & Wu, X. R. (2018). Downhole geothermal power generation in oil and gas wells. *Geothermics* **76**, 141-148.

Wang, Z., McClure, M. & Horne, R. (2009). A single-well EGS configuration using a thermosiphon. *Workshop on geothermal reservoir engineering*. Stanford University, Stanford, California.

Willhite, G. P. (1967). Over-all heat transfer coefficients in steam and hot water injection wells. *Journal of Petroleum Technology* **19**, 607-615.